

Intelligent Firefly Algorithm Deep Transfer Learning Based COVID-19 Monitoring System

Mahmoud Ragab^{1,2,3,*}, Mohammed W. Al-Rabia^{4,5}, Sami Saeed Binyamin⁶ and Ahmed A. Aldarmahi^{7,8}

¹Information Technology Department, Faculty of Computing and Information Technology, King Abdulaziz University, Jeddah 21589, Saudi Arabia

²Centre for Artificial Intelligence in Precision Medicines, King Abdulaziz University, Jeddah 21589, Saudi Arabia

³Mathematics Department, Faculty of Science, Al-Azhar University, Naser City 11884, Cairo, Egypt

⁴Department of Medical Microbiology and Parasitology, Faculty of Medicine, King Abdulaziz University, Jeddah 21589, Saudi Arabia

⁵Health Promotion Center, King Abdulaziz University, Jeddah 21589, Saudi Arabia

⁶Computer and Information Technology Department, The Applied College, King Abdulaziz University, Jeddah 21589, Saudi Arabia

⁷Basic Science Department, College of Science and Health Professions,

King Saud Bin Abdulaziz University for Health Sciences, Jeddah 21423, Saudi Arabia

⁸King Abdullah International Medical Research Center, Ministry of National Guard-Health Affairs, Jeddah 21423, Saudi Arabia

*Corresponding Author: Mahmoud Ragab. Email: mragab@kau.edu.sa

Received: 10 May 2022; Accepted: 10 June 2022

Abstract: With the increasing and rapid growth rate of COVID-19 cases, the healthcare scheme of several developed countries have reached the point of collapse. An important and critical steps in fighting against COVID-19 is powerful screening of diseased patients, in such a way that positive patient can be treated and isolated. A chest radiology image-based diagnosis scheme might have several benefits over traditional approach. The accomplishment of artificial intelligence (AI) based techniques in automated diagnoses in the healthcare sector and rapid increase in COVID-19 cases have demanded the requirement of AI based automated diagnosis and recognition systems. This study develops an Intelligent Firefly Algorithm Deep Transfer Learning Based COVID-19 Monitoring System (IFFA-DTLMS). The proposed IFFA-DTLMS model majorly aims at identifying and categorizing the occurrence of COVID19 on chest radiographs. To attain this, the presented IFFA-DTLMS model primarily applies densely connected networks (DenseNet121) model to generate a collection of feature vectors. In addition, the firefly algorithm (FFA) is applied for the hyper parameter optimization of DenseNet121 model. Moreover, autoencoder-long short term memory (AE-LSTM) model is exploited for the classification and identification of COVID19. For ensuring the enhanced performance of the IFFA-DTLMS model, a wide-ranging experiments were performed and the results are reviewed under distinctive aspects. The experimental value reports the betterment of IFFA-DTLMS model over recent approaches.



This work is licensed under a Creative Commons Attribution 4.0 International License, which permits unrestricted use, distribution, and reproduction in any medium, provided the original work is properly cited.

Keywords: COVID-19; artificial intelligence; intelligent systems; deep learning; decision making

1 Introduction

Nowadays, the COVID-19 outbreak is considered as a universal problem confronted by healthcare administrations. From November 19, 2020, the overall quantity of individuals globally who confirmed that they were affected with SARS-COV-2 was above 56.4 million, whereas the total quantity of mortality from the COVID-19 is exceeding 1.35 million, so showing that coronavirus infections were increasing globally [1]. The patients who are affected by COVID-19 have numerous symptoms, like decrease in oxygen saturation level, fever, body pain, diarrhea, dry cough, shortness of breath, loss of taste and smell, vomiting, and abnormal pulse rate, headache, and sore throat [2]. Amid such indications, low oxygen saturation level, abnormal pulse rate, and high fever were concerned as serious. Shortness of breath and low oxygen saturation level leads to hypoxia and hypoxemia. Patients suffer from hypoxemia and difficulties with heartbeat are of less chance of living [3]. In some cases, patients will not identify hypoxia and a rising pulse rate and become disease by not having appropriate medication. Non-invasive healthcare can be the only possible means to lower the spreading of virus effectively. Technologies were quickly advancing currently and non-invasive healthcare has grabbed the interest of several researchers worldwide alleviating the work pressure on health labors [4]. Also, the progression of healthcare technologies might substantially diminish the amount of useful clinical sources.

An automatic health monitoring module was enhanced which creates a warning in the serious situation of the patient [5]. A chest radiology image-oriented detection technique could prevail numerous benefits rather than classical techniques. It is quick, to examine many cases concurrently, has better accessibility, and most significantly this technique is more helpful in clinics not having few or restricted testing kits and sources [6,7]. Also, providing significance of radiography in latest healthcare scheme, radiology imaging system was existing in all clinics, thus makes radiography-related techniques easily available and very convenient. Authors are aiming at deep learning (DL) methods for identifying certain particular features from chest radiography images of COVID19 cases [8]. Recently, DL made successful accomplishments in several visual tasks that also involves medical image examination. DL has transformed automated disease prognosis and administration by precisely identifying examining, and categorizing paradigms in healthcare images [9,10]. The motive behind this accomplishment is DL methods do not depend on automatic hand-engineered features but such methods study features mechanically through information itself.

Hassantabar et al. [11] employed 3 DL-related techniques for the identification and detection of coronavirus patient using X-Ray images of lungs. For the disease diagnosis, there are 2 methods that are CNN and DNN on the fractal feature of images methodologies by using lung images, straightforwardly. Rasheed et al. [12] inspected the efficiency of ML methodologies for automated prognosis of coronavirus with higher accurateness from X-ray images. Two frequently utilized classifiers have been chosen one is CNN and another one is logistic regression (LR). The first and foremost reason is to make the scheme faster and more effective. Additionally, a dimension reduction method has been inspected grounded on PCA to additionally fasten the process of learning and improve the categorization accuracy through choosing the extremely discriminative feature.

In [13], an original DL-related system, known as COVID-XNet, was exhibited for coronavirus prognosis in chest X-ray images. The presented technique executes a set of preprocessing methods to the input image for variability reduction and contrast enhancement that are fed to a custom CNN

for extracting appropriate features and accomplishing the categorization among normal cases and coronavirus. In [14], a novel method for automatic COVID19 recognition with the help of raw chest X-ray images was submitted. The presented method has been enhanced to offer precise diagnostics for multi-class and binary categorization. The DarkNet method can be utilized in this article as a classification for you-only-look-once (YOLO) real time object recognition module. Yoo et al. [15] examine the possibility of utilizing a DL-related decision-tree classifier for recognizing COVID19 from CXR images. The suggested classifier has 3 binary DTs, all of these are trained by a DL method with CNN related method on the PyTorch frame. The primary DT categorizes the CXR images into abnormal or normal. Almalki et al. [16] recommend an original methodology CoVIRNet (COVID Inception-ResNet model), that uses the chest X-rays for diagnosing the coronavirus patient mechanically. The suggested method contains distinct inception residual blocks which cater to information with the help of distinct depth feature mappings at diverse scales, with several layers. The features were concatenated at every suggested classification block, with the help of the average pooling layer, and concatenated feature was passed to the completely linked layer.

This study develops an Intelligent Firefly Algorithm Deep Transfer Learning Based COVID-19 Monitoring System (IFFA-DTLMS). The proposed IFFA-DTLMS model primarily applies densely connected networks (DenseNet121) model to produce a collection of feature vectors. In addition, the firefly algorithm (FFA) is applied for hyper parameter optimization of the DenseNet121 architecture. Moreover, Autoencoder-LSTM (AE-LSTM) model is exploited for the diagnosis and classification of COVID-19. For ensuring the enhanced performance of the IFFA-DTLMS model, a wide range of experiments were performed and the outcomes are reviewed under distinctive aspects.

The rest of the paper is organized as follows. Section 2 offers the proposed model, Section 3 validates the performance, and Section 4 concludes the study.

2 The Proposed Model

In this study, a new IFFA-DTLMS model was designed to categorize and identify the occurrence of COVID-19 on chest radiographs. The presented IFFA-DTLMS model primarily applied DenseNet121 model to generate a collection of feature vectors. In addition, the FFA is applied for hyper parameter optimization of the DenseNet121 model. Moreover, AE-LSTM model is exploited for the diagnosis and classification of COVID-19.

2.1 DenseNet Feature Extraction

In this work, the presented IFFA-DTLMS model primarily applied DenseNet121 model to generate a collection of feature vectors. The DenseNet-121 framework is applied as the baseline in this study. Also, transfer learning model takes place in DenseNet module to augment the efficiency of system [17]. In contrast to DenseNet, it needs fewer parameters than that of classical CNN model because they don't need to learn unwanted feature maps. The fundamental concept of DenseNet structure is the feature reutilization that leads to highly compact form. Subsequently, it requests fewer parameters than that of other CNN models because no feature map is reiterated. When CNN goes further, they face problems. DenseNet makes the connectivity far simpler by easily connecting each layer with other layers. DenseNet utilizes the network ability by reusing features. Fig. 1 depicts the framework of DenseNet. Every single layer in DenseNet obtains input over each preceding layer and transfers feature map to the subsequent layer.

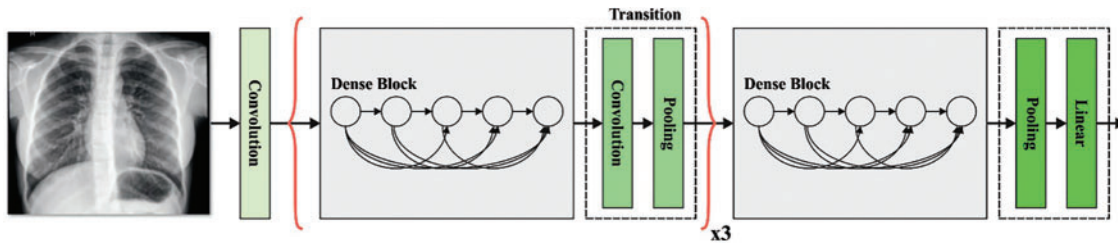


Figure 1: Structure of DenseNet

2.2 Hyperparameter Optimization

Here, the FFA is applied for hyperparameter optimization of the DenseNet121 model. The FFA was initially developed by Yang in [18]. This popular approach has been stimulated by flashing characteristics and social behavior. Because the real-time firefly ecosystem is sophisticated and very complex, the FFA metaheuristic is their calculation. The real formula of attraction is a critical problem that needs to be tackled in the execution of FFA. Generally, the attraction of firefly is depending on the brightness that sequentially depends on the decision criterion. For minimization problem, the brightness of firefly on the x position is evaluated as follows:

$$I(x) = \begin{cases} \frac{1}{f(x)}, & \text{if } f(x) > 0 \\ 1 + |f(x)|, & \text{or else} \end{cases} \quad (1)$$

In Eq. (1), $I(x)$ indicates the attraction, and $f(x)$ characterize the value of decision criterion at the x position. It is evident that Eq. (10) signifies fitness function. When we detect arithmetical features, attractiveness and light intensity are continually lessening function, when the distance from the light source rises, attractiveness and light intensity would decrease. It is formulated in the following expression:

$$I(r) = \frac{I_0}{1 + \gamma r^2} \quad (2)$$

In Eq. (2), $I(r)$ indicates the light intensity, r symbolizes the distance, and I_0 denotes the intensity of light at the source position. Furthermore, light is absorbed partly by the adjacent air, which causes light to turn out to be weak. Such occurrences are demonstrated through the light absorption coefficient γ . Based on the study, nearly every implementation of the FFA considered the influence of the inverse square law on the absorption and distance of light, by approaching the subsequent Gaussian formulation:

$$I(r) = I_0 \cdot e^{-\gamma r^2} \quad (3)$$

Attractiveness β of firefly individuals is relatively based on the distance among the target and the observer fireflies. Simultaneously, the attractiveness is straight proportionate to the light intensity that is estimated by the following expression:

$$\beta(r) = \beta_0 \cdot e^{-\gamma r^2} \quad (4)$$

In Eq. (4), the β_0 variable indicates the attraction at distance $r = 0$. Also, it assists to determine the distance $\gamma = 1/\sqrt{\gamma}$ whereby the attraction of fireflies significantly changes from β_0 to $\beta_0 e^{-1}$. It is frequently substituted with the following equation:

$$\beta(r) = \frac{\beta_0}{1 + \gamma r^2} \tag{5}$$

The subjective firefly i move towards the novel location (in the $t + 1$ following iteration) to the brightness, attractive firefly j , is formulated by:

$$x_i^{t+1} = x_i^t + \beta_0 \cdot e^{-\gamma r_{ij}^2} (x_j^t - x_i^t) + \alpha^t (\kappa - 0.5) \tag{6}$$

where para

$$x_i^{t+1} = x_i^t + \beta_0 \cdot e^{-\gamma r_{ij}^2} (x_j^t - x_i^t) + \alpha^t (\kappa - 0.5) \tag{7}$$

In which, β_0 parameter represents the attraction towards distance $r = 0$, α denotes a randomized variable, κ indicates an arbitrary integer derived from Gaussian or uniform distribution, r_{ij} characterizes the distance amongst i and j . The position of FF is sequentially upgraded, by updating and comparison of all the pairs of FF in all the iterations. The distance among i and j is evaluated by the Cartesian distance:

$$r_{i,j} = ||x_i - x_j|| = \sqrt{\sum_{k=1}^D (x_{i,k} - x_{j,k})^2} \tag{8}$$

In Eq. (8), D indicates the parameter number. The suitable value for problem is $\beta_0 = 1$ and $\alpha \in [0, 1]$. Fig. 2 demonstrates the flowchart of FFA.

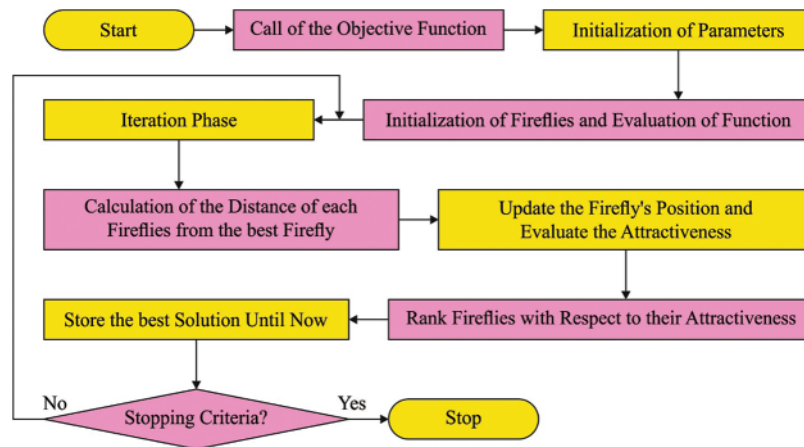


Figure 2: Flowchart of FFA

The FFA approach develops a fitness function (FF) for gaining higher classifier performances. It solves a positive integer for demonstrating the best performance of solution candidate. In such cases, the minimized classifier error rate is considered as FF in Eq. (9). A worst outcome gains an improved error rate and best possible solution attains a lesser error rate.

$$fitness(x_i) = ClassifierErrorRate(x_i) = \frac{number\ of\ misclassified\ samples}{Total\ number\ of\ samples} * 100 \tag{9}$$

2.3 AE-LSTM Based Classification

In the final step, the AE-LSTM model is exploited for the diagnosis and classification of COVID-19. The LSTM model is superior RNN that is initially developed. RNN is a neural network (NN)

with recurring relationships among the neurons which allows them to learn from the previous and the current dataset for finding a good outcome [19]. But once the two cells in RNN are farther from one another, it is complex to attain valuable dataset as a result of the gradient explosion and vanishing issues. The solution to this is distinctive neuron termed memory cell. With this neuron, the LSTM is capable of storing effective dataset within a certain duration. Furthermore, LSTM cell is capable of learning what information must be erased, read, and stored from the memory by regulating three dissimilar controlled gates, such as output gate ($o(t)$), forget gate ($f(t)$), and input gate ($i(t)$). The forget gate ($f(t)$) determines to discard or keep the dataset from the cell state, demonstrated in Eq. (10). A logistical function produces whether zero or one value for $f(t)$ which indicates retaining or abandon the existing state of the cell in t time, correspondingly. In which b , w , h , and x , indicate the bias, weight, output, and input, correspondingly. The activation function is characterized as σ . Alternatively, the input gate deals with input value which is saved in the cell state. While $i(t)$ signifies the signal (0 or 1) which controls the update process, $g(t)$ indicates a novel candidate value and $c(t)$ indicates the novel cell state. Additionally, the output gate ($o(t)$) is accountable to release the saved dataset for the following neuron. Therefore, LSTM is an effective ML methodology for capturing the non-linear relationship and long-term dependency in complicated data.

$$f(t) = \sigma(w_f[h(t-1), x(t)] + b_f) \quad (10)$$

$$c(t) = f(t)*c(t-1) + i(t)*g(t) \quad (11)$$

$$i(t) = \sigma(w_i[h(t-1), x(t)] + b_i) \quad (12)$$

$$g(t) = \tanh(w_g[h(t-1), x(t)] + b_g) \quad (13)$$

$$o(t) = \sigma(w_o[h(t-1), x(t)] + b_o) \quad (14)$$

$$h(t) = o(t)*\tanh(c(t)) \quad (15)$$

The AE-LSTM developed comprises LSTM and AE [20]. An AE is an unsupervised neural network in which output and input layers possess similar sizes. AE tries to acquire the individuality function such that the x input is almost analogous to the \hat{x} output with certain limitations that is, limited neuron count in the hidden state than that of the input unit. Consequently, an AE performs as a compressor and a decompressor containing two parts as follows:

Solar power generation predicting

- (i) Encoder, wherein the layer is decreased from input to the hidden states and
- (ii) Decoder, wherein the neuron in the encoder are imitated.

Consequently, an AE is capable of learning and discovering the connections in the input feature and the distinct architecture of the dataset. The ending outcome of AE-LSTM is an ML technique which is capable of predicting the occurrence of COVID19 by means of input image.

3 Results and Discussion

The experimental validation of the IFFA-DTLMS model is tested using the CXR image dataset [21], containing 32224 samples under COVID and 6448 samples under healthy class. A few image samples are illustrated in Fig. 3.

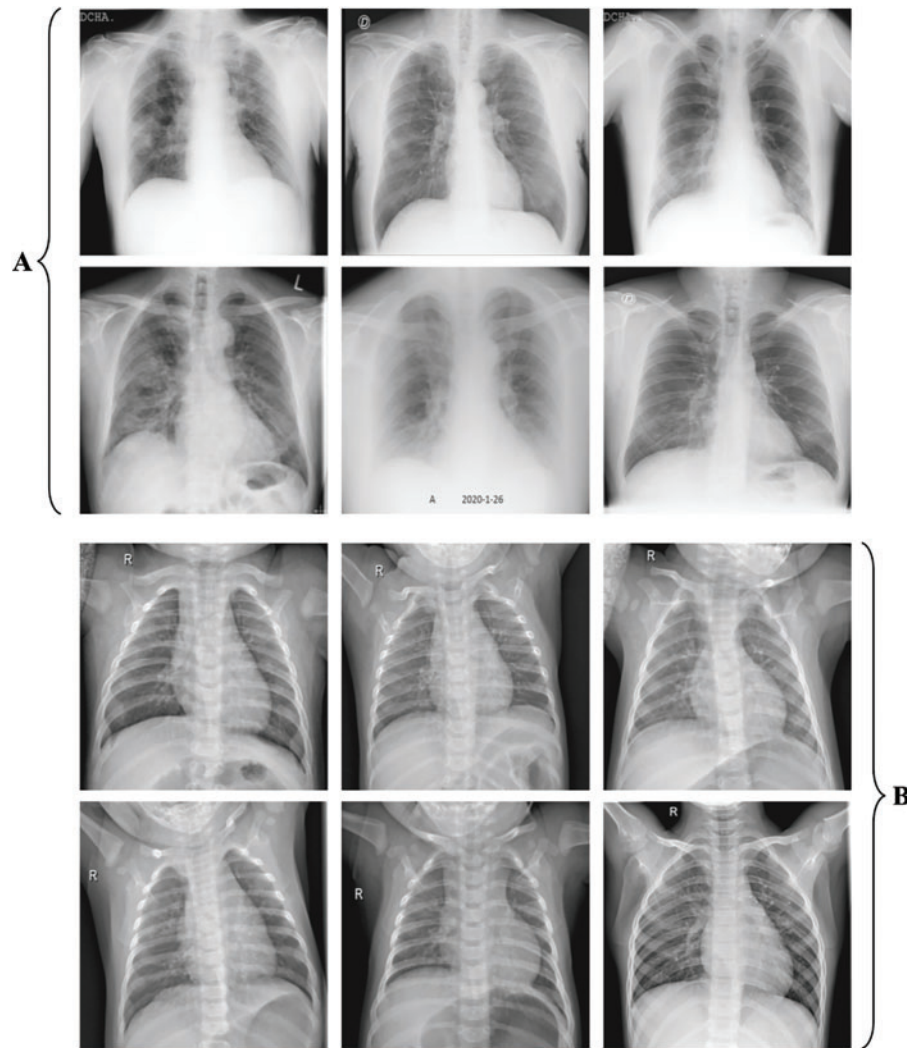


Figure 3: a) COVID b) Healthy

The confusion matrix produced by the IFFA-DTLMS model on the testing dataset is depicted in Fig. 4. On run-1, the IFFA-DTLMS model has recognized 3168 samples into COVID and 3177 samples under healthy. Also, on run-3, the IFFA-DTLMS technique has recognized 3194 samples into COVID and 3146 samples under healthy. Besides, on run-5, the IFFA-DTLMS approach has recognized 3188 samples into COVID and 3153 samples under healthy.

Tab. 1 and Fig. 5 highlight the overall analysis result of the IFFA-DTLMS model on the testing data. The results portrayed that the IFFA-DTLMS model has reached enhanced performance under every run. For example, on run-1, the IFFA-DTLMS model has provided enhanced average $accu_y$, $prec_n$, $reca_l$, $spec_y$, F_{score} , and MCC of 98.40%, 98.40%, 98.40%, 98.40%, 98.40%, and 96.81% respectively. Likewise, on run-3, the IFFA-DTLMS system has presented enhanced average $accu_y$, $prec_n$, $reca_l$, $spec_y$, F_{score} , and MCC of 98.33%, 98.34%, 98.33%, 98.33%, 98.32%, and 96.66% correspondingly. Moreover, on run-5, the IFFA-DTLMS methodology has offered enhanced average $accu_y$, $prec_n$, $reca_l$, $spec_y$, F_{score} , and MCC of 98.34%, 98.35%, 98.34%, 98.34%, 98.34%, and 96.69% correspondingly.

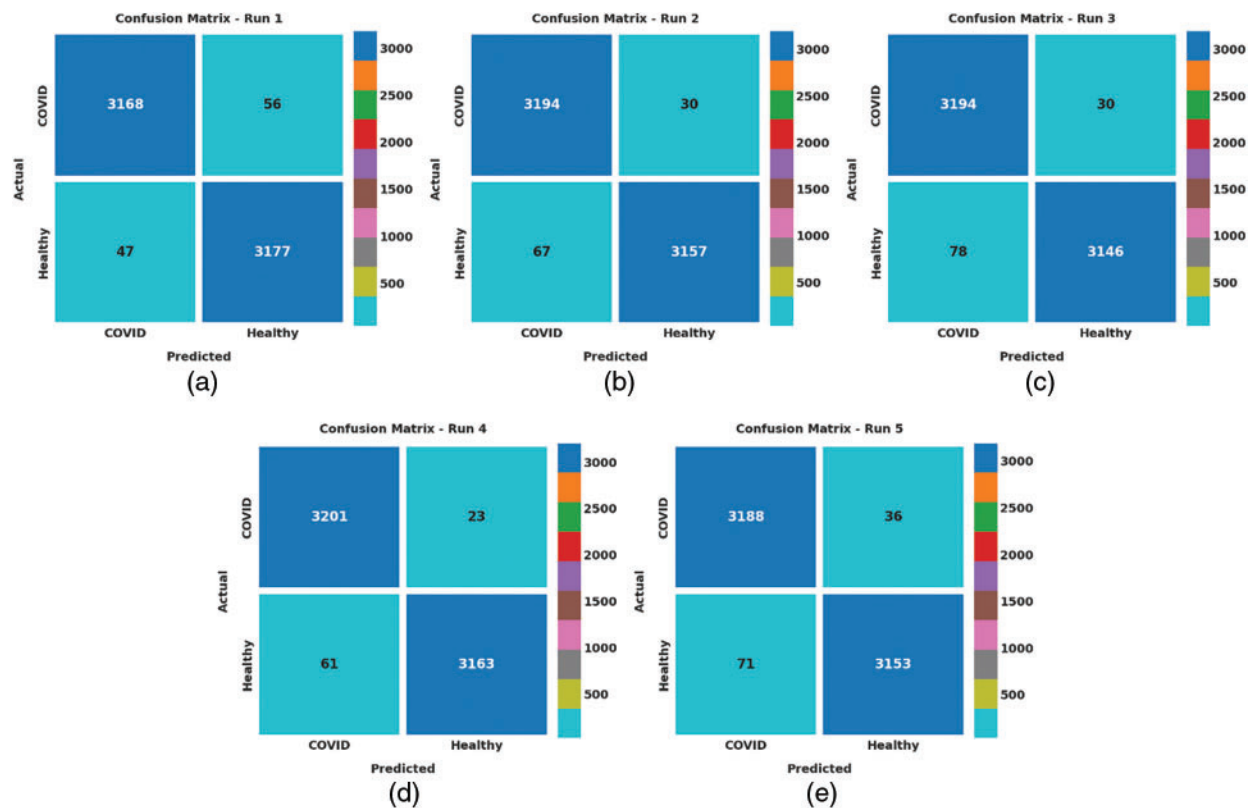


Figure 4: Confusion matrices of IFFA-DTLMS technique (a) Run-1, (b) Run-2, (c) Run-3, (d) Run-4, and (e) Run-5

Table 1: Analysis result of IFFA-DTLMS approach with various measures and runs

Labels	Accuracy	Precision	Recall	Specificity	F-score	MCC
Run-1						
COVID	98.40	98.54	98.26	98.54	98.40	96.81
Healthy	98.40	98.27	98.54	98.26	98.40	96.81
Average	98.40	98.40	98.40	98.40	98.40	96.81
Run-2						
COVID	98.50	97.95	99.07	97.92	98.50	97.00
Healthy	98.50	99.06	97.92	99.07	98.49	97.00
Average	98.50	98.50	98.50	98.50	98.50	97.00
Run-3						
COVID	98.33	97.62	99.07	97.58	98.34	96.66
Healthy	98.33	99.06	97.58	99.07	98.31	96.66
Average	98.33	98.34	98.33	98.33	98.32	96.66

(Continued)

Table 1: Continued

Labels	Accuracy	Precision	Recall	Specificity	F-score	MCC
Run-4						
COVID	98.70	98.13	99.29	98.11	98.70	97.40
Healthy	98.70	99.28	98.11	99.29	98.69	97.40
Average	98.70	98.70	98.70	98.70	98.70	97.40
Run-5						
COVID	98.34	97.82	98.88	97.80	98.35	96.69
Healthy	98.34	98.87	97.80	98.88	98.33	96.69
Average	98.34	98.35	98.34	98.34	98.34	96.69

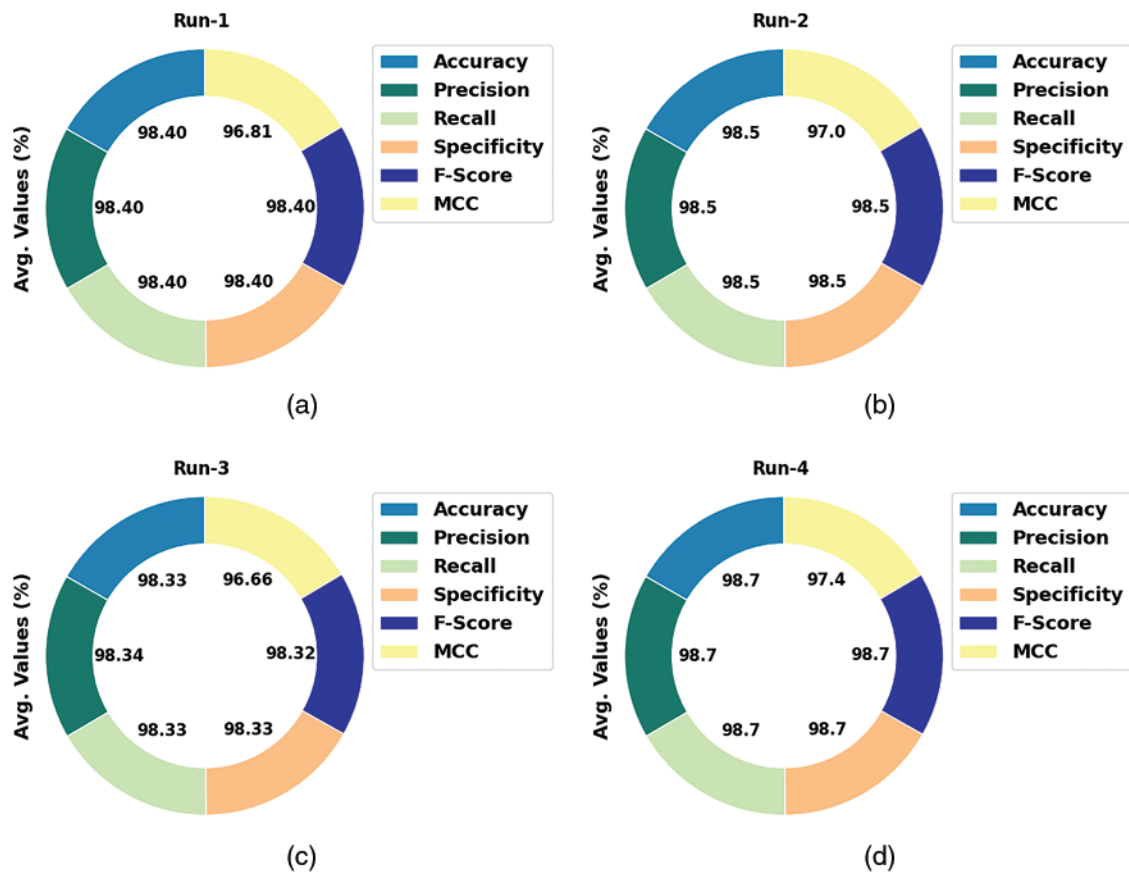


Figure 5: (Continued)

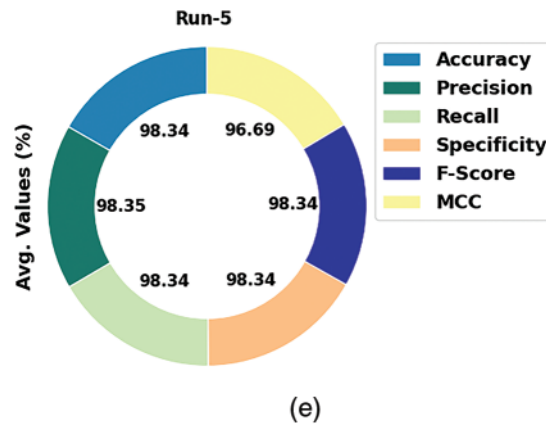


Figure 5: Average analysis of IFFA-DTLMS method (a) Run-1, (b) Run-2, (c) Run-3, (d) Run-4, and (e) Run-5

The training accuracy (TA) and validation accuracy (VA) attained by the IFFA-DTLMS approach on testing data is illustrated in Fig. 6. The experimental outcome implied that the IFFA-DTLMS system has acquired maximum values of TA and VA. In specific, the VA seemed to be higher than TA.

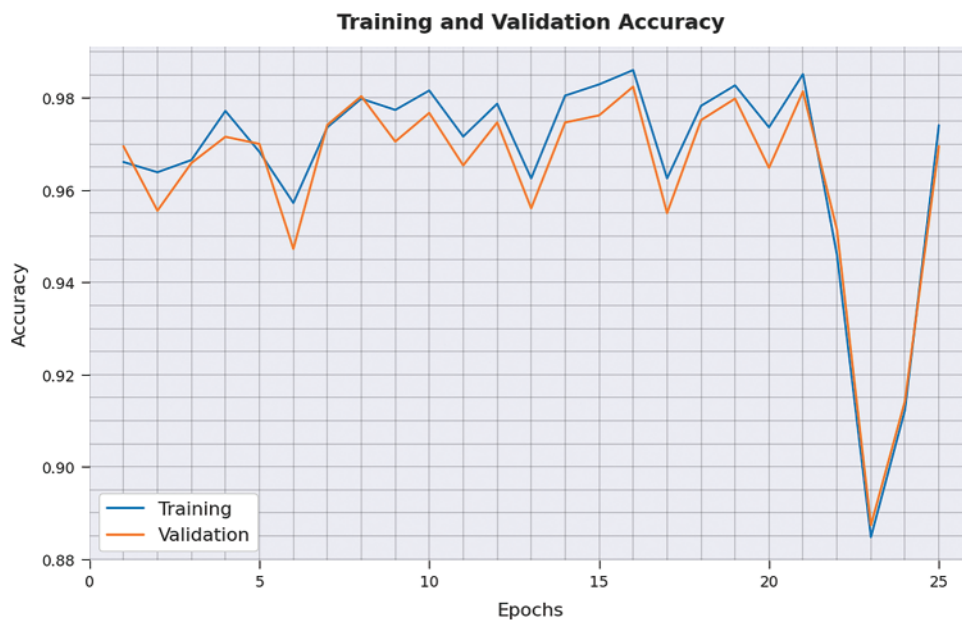


Figure 6: TA and VA analysis of IFFA-DTLMS approach

The training loss (TL) and validation loss (VL) achieved by the IFFA-DTLMS methodology on test dataset are established in Fig. 7. The experimental outcome inferred that the IFFA-DTLMS approach has established least values of TL and VL. In specific, the VL seemed to be lesser than TL.

A brief precision-recall inspection of the IFFA-DTLMS method on test dataset is represented in Fig. 8. By observing the figure, it is noticed that the IFFA-DTLMS model has established maximum precision-recall performance under distinct classes.



Figure 7: TL and VL analysis of IFFA-DTLMS approach

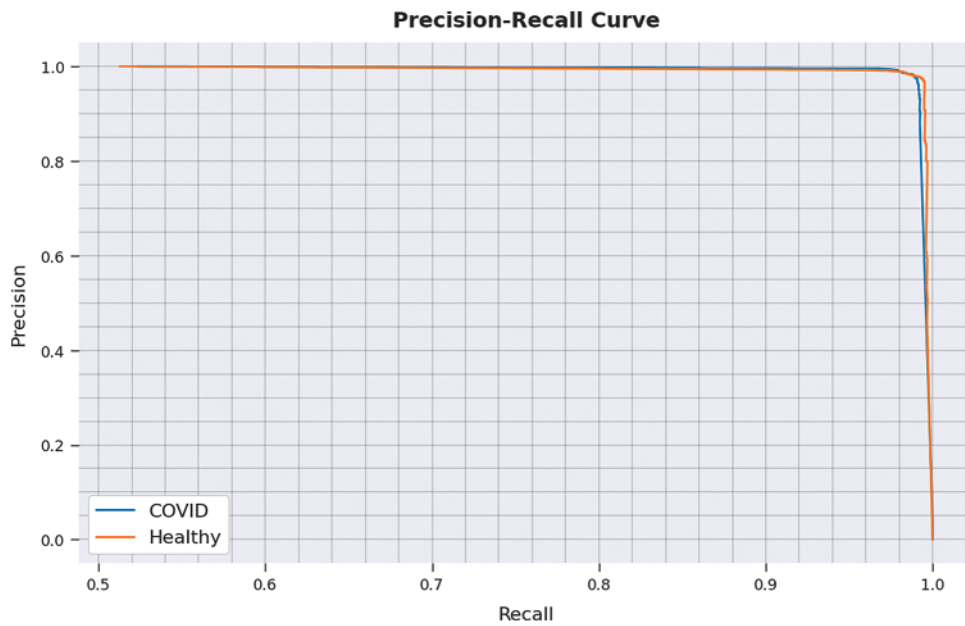


Figure 8: Precision-recall curve analysis of IFFA-DTLMS approach

A detailed ROC investigation of the IFFA-DTLMS methodology on test data is portrayed in Fig. 9. The results specified that the IFFA-DTLMS system has shown its ability in categorizing two distinct classes on test dataset.

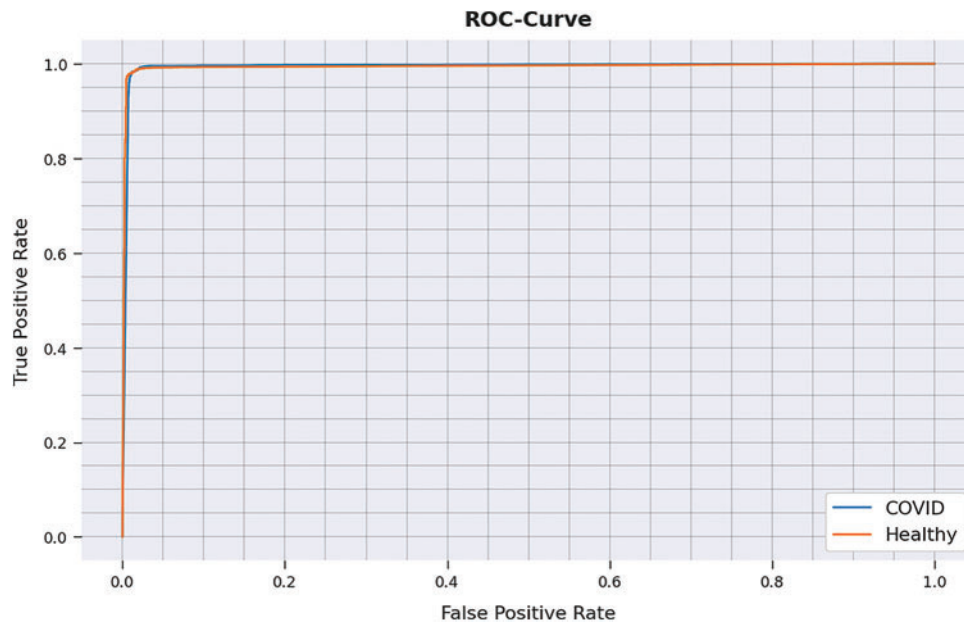


Figure 9: ROC curve analysis of IFFA-DTLMS approach

Tab. 2 illustrates a comparative study of IFFA-DTLMS model with existing models [22–26].

Table 2: Comparative analysis of IFFA-DTLMS technique with existing techniques

Methods	Precision	Sensitivity	Specificity	Accuracy	F-score	MCC
DBHL	97.32	97.98	98.54	98.43	98.19	97.27
DHL-2	96.10	98.45	96.88	98.04	98.41	97.10
DHL-1	97.25	98.20	98.34	97.93	97.58	95.21
ResNet-2	97.07	97.41	97.26	97.25	96.41	93.61
TL-ResNet-2	97.81	97.83	97.28	98.54	97.22	95.54
ResNet-1	96.53	96.45	97.50	97.40	96.79	93.71
TL-RENet-1	98.37	97.77	98.16	97.54	98.26	96.01
IFFA-DTLMS	98.70	98.70	98.70	98.70	98.70	97.40

Fig. 10 reports a comparison study of the IFFA-DTLMS model with other models in terms of $prec_n$, $reca_1$, and $accu_y$. The figure implied that the IFFA-DTLMS model has gained effectual outcomes over other models. With respect to $prec_n$, the IFFA-DTLMS model has offered higher $prec_n$ of 98.70% whereas the DBHL, DHL-2, DHL-1, ResNet-2, TL-ResNet-2, ResNet-1, and TL-RENet-1 models have attained reduced $prec_n$ of 97.32%, 96.10%, 97.25%, 97.07%, 97.81%, 96.53%, and 98.37% respectively. Also, with respect to $accu_y$, the IFFA-DTLMS method has provided higher $accu_y$ of 98.70% whereas the DBHL, DHL-2, DHL-1, ResNet-2, TL-ResNet-2, ResNet-1, and TL-RENet-1 approaches have acquired reduced $accu_y$ of 98.43%, 98.04%, 97.93%, 97.25%, 98.54%, 97.40%, and 97.54% correspondingly.

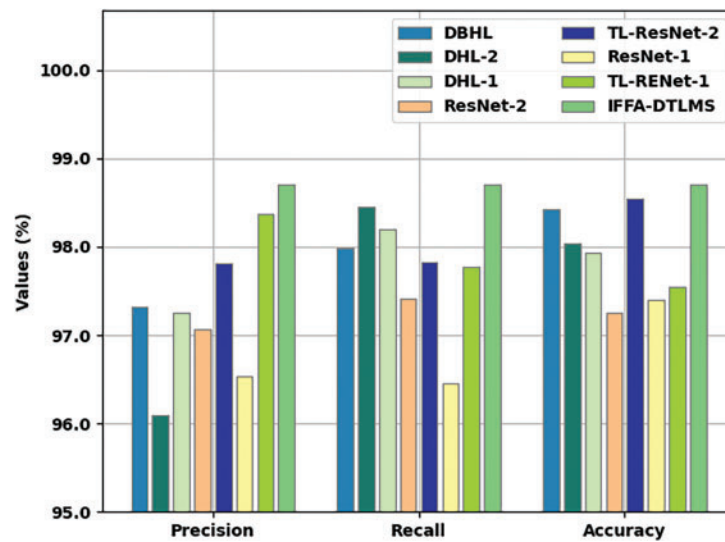


Figure 10: $Prec_n$, $reca_l$, and $accu_y$ analysis of IFFA-DTLMS algorithm with recent methods

Fig. 11 reports a comparison study of the IFFA-DTLMS method with other models interms of $spec_y$, F_{score} , and MCC. The figure implied that the IFFA-DTLMS system has acquired effectual outcomes over other models. In relation to $spec_y$, the IFFA-DTLMS system has provided higher $spec_y$ of 98.70% whereas the DBHL, DHL-2, DHL-1, ResNet-2, TL-ResNet-2, ResNet-1, and TL-RENet-1 techniques have gained reduced $spec_y$ of 98.54%, 96.88%, 98.34%, 97.26%, 97.28%, 97.50%, and 98.16% correspondingly. Likewise, with regard to MCC, the IFFA-DTLMS method has rendered higher MCC of 97.40% whereas the DBHL, DHL-2, DHL-1, ResNet-2, TL-ResNet-2, ResNet-1, and TL-RENet-1 algorithms have gained reduced MCC of 97.27%, 97.10%, 95.21%, 93.61%, 95.54%, 93.71%, and 96.01% correspondingly. Therefore, it is confirmed that the IFFA-DTLMS model has showcased improved performance over the existing approaches.

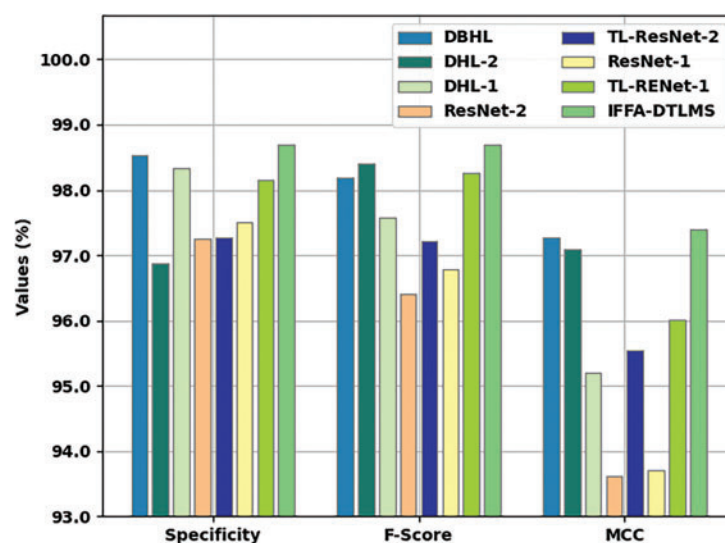


Figure 11: $Spec_y$, F_{score} , and MCC analysis of IFFA-DTLMS algorithm with recent methods

4 Conclusion

In this study, a new IFFA-DTLMS model was designed to categorize and identify the occurrence of COVID-19 on chest radiographs. The presented IFFA-DTLMS model primarily applied DenseNet121 model to generate a collection of feature vectors. In addition, the FFA is applied for hyper parameter optimization of the DenseNet121 model. Moreover, AE-LSTM model is exploited for the diagnosis and classification of COVID-19. For ensuring the enhanced performance of the IFFA-DTLMS model, a wide-ranging experiment were performed and the results are inspected under distinct aspects. The experimental value reports the betterment of IFFA-DTLMS model over recent approaches. In the context of future development, the presented IFFA-DTLMS model can be extended to the utilization of computed tomography (CT) images.

Funding Statement: This work was funded by the Deanship of Scientific Research (DSR), King Abdulaziz University, Jeddah, under grant no. (G: 366-140-38). The authors gratefully acknowledge DSR technical and financial support.

Conflicts of Interest: The authors declare that they have no conflicts of interest to report regarding the present study.

References

- [1] A. Borkowski, "Using artificial intelligence for covid-19 chest x-ray diagnosis," *Federal Practitioner*, vol. 37, no. 9, pp. 398–404, 2020.
- [2] R. Yasin and W. Gouda, "Chest X-ray findings monitoring COVID-19 disease course and severity," *Egyptian Journal of Radiology and Nuclear Medicine*, vol. 51, no. 1, pp. 193, 2020.
- [3] A. I. Khan, J. L. Shah and M. M. Bhat, "CoroNet: A deep neural network for detection and diagnosis of COVID-19 from chest x-ray images," *Computer Methods and Programs in Biomedicine*, vol. 196, no. 2020, pp. 1–9, 2020.
- [4] L. A. Rousan, E. Elobeid, M. Karrar and Y. Khader, "Chest x-ray findings and temporal lung changes in patients with COVID-19 pneumonia," *BMC Pulmonary Medicine*, vol. 20, no. 1, pp. 1–17, 2020.
- [5] A. Borghesi and R. Maroldi, "COVID-19 outbreak in Italy: Experimental chest X-ray scoring system for quantifying and monitoring disease progression," *Radiol Med.*, vol. 125, no. 5, pp. 509–513, 2020, <https://doi.org/10.1007/s11547-020-01200-3>.
- [6] S. Tabik, A. G. Ríos, J. L. M. Rodríguez, I. S. García, M. R. Area *et al.*, "COVIDGR dataset and covid-sdnet methodology for predicting covid-19 based on chest x-ray images," *IEEE Journal of Biomedical and Health Informatics*, vol. 24, no. 12, pp. 3595–3605, 2020.
- [7] E. Benmalek, J. Elmhamdi and A. Jilbab, "Comparing CT scan and chest X-ray imaging for COVID-19 diagnosis," *Biomedical Engineering Advances*, vol. 1, no. 2021, pp. 1–6, 2021.
- [8] X. Qi, L. G. Brown, D. J. Foran, J. Noshier and I. Hacihaliloglu, "Chest X-ray image phase features for improved diagnosis of COVID-19 using convolutional neural network," *International Journal of Computer Assisted Radiology and Surgery*, vol. 16, no. 2, pp. 197–206, 2021.
- [9] M. Turkoglu, "COVIDetectioNet: COVID-19 diagnosis system based on X-ray images using features selected from pre-learned deep features ensemble," *Applied Intelligence*, vol. 51, no. 3, pp. 1213–1226, 2021.
- [10] K. K. Singh, M. Siddhartha and A. Singh, "Diagnosis of coronavirus disease (COVID-19) from chest X-ray images using modified XceptionNet," *Romanian Journal of Information Science and Technology*, vol. 23, no. 657, pp. 91–115, 2020.
- [11] S. Hassantabar, M. Ahmadi and A. Sharifi, "Diagnosis and detection of infected tissue of COVID-19 patients based on lung x-ray image using convolutional neural network approaches," *Chaos, Solitons & Fractals*, vol. 140, pp. 1–11, 2020.

- [12] J. Rasheed, A. A. Hameed, C. Djeddi, A. Jamil and F. Al-Turjman, "A machine learning-based framework for diagnosis of COVID-19 from chest X-ray images," *Interdisciplinary Sciences: Computational Life Science*, vol. 13, no. 1, pp. 103–117, 2021.
- [13] L. D. Lopez, J. P. D. Morales, J. C. Jaime, S. V. Diaz and A. L. Barranco, "COVID-XNet: A custom deep learning system to diagnose and locate covid-19 in chest x-ray images," *Applied Sciences*, vol. 10, no. 16, pp. 5683, 2020.
- [14] T. Ozturk, M. Talo, E. A. Yildirim, U. B. Baloglu, O. Yildirim *et al.*, "Automated detection of COVID-19 cases using deep neural networks with X-ray images," *Computers in Biology and Medicine*, vol. 121, pp. 103792, 2020.
- [15] S. H. Yoo, H. Geng, T. L. Chiu, S. K. Yu, D. C. Cho *et al.*, "Deep learning-based decision-tree classifier for covid-19 diagnosis from chest x-ray imaging," *Frontiers in Medicine*, vol. 7, pp. 427, 2020.
- [16] Y. E. Almalki, A. Qayyum, M. Irfan, N. Haider, A. Glowacz *et al.*, "A novel method for covid-19 diagnosis using artificial intelligence in chest x-ray images," *Healthcare*, vol. 9, no. 5, pp. 1–12, 2021.
- [17] T. Chauhan, H. Palivela and S. Tiwari, "Optimization and fine-tuning of DenseNet model for classification of COVID-19 cases in medical imaging," *International Journal of Information Management Data Insights*, vol. 1, no. 2, pp. 1–12, 2021.
- [18] X. S. Yang, "Firefly algorithm, stochastic test functions and design optimisation," *International Journal of Bio-Inspired Computation*, vol. 2, no. 2, pp. 1–12, 2010.
- [19] J. Zheng, C. Xu, Z. Zhang and X. Li, "Electric load forecasting in smart grids using long-short-term-memory based recurrent neural network," in *2017 51st Annual Conf. on Information Sciences and Systems (CISS)*, Baltimore, MD, USA, pp. 1–6, 2017.
- [20] A. Sagheer and M. Kotb, "Unsupervised pre-training of a deep lstm-based stacked autoencoder for multivariate time series forecasting problems," *Scientific Reports*, vol. 9, no. 1, pp. 19038, 2019.
- [21] "Dataset: <https://github.com/ieee8023/covid-chestxray-dataset>.
- [22] M. Ragab, S. Alshehri, N. Alhakamy, W. Alsaggaf, H. Alhadrami *et al.*, "Machine learning with quantum seagull optimization model for covid-19 chest x-ray image classification," *Journal of Healthcare Engineering*, vol. 2022, pp. 1–13, 2022.
- [23] R. F. Mansour, J. E. Gutierrez, M. Gamarra, D. Gupta, O. Castillo *et al.*, "Unsupervised deep learning based variational autoencoder model for covid-19 diagnosis and classification," *Pattern Recognition Letters*, vol. 151, pp. 267–274, 2021.
- [24] K. Shankar, E. Perumal, M. Elhoseny, F. Taher, B. B. Gupta *et al.*, "Synergic deep learning for smart health diagnosis of covid-19 for connected living and smart cities," *ACM Transactions on Internet Technology*, vol. 22, no. 3, pp. 1–14, 2022.
- [25] K. Shankar, E. Perumal, P. Tiwari, M. Shorfuzzaman and D. Gupta, "Deep learning and evolutionary intelligence with fusion-based feature extraction for detection of COVID-19 from chest X-ray images," *Multimedia Systems*, 2021, <https://doi.org/10.1007/s00530-021-00800-x>.
- [26] K. Shankar, E. Perumal, V. G. Díaz, P. Tiwari, D. Gupta *et al.*, "An optimal cascaded recurrent neural network for intelligent COVID-19 detection using chest X-ray images," *Applied Soft Computing*, vol. 113, pp. 107878, 2021.